Compressing μJ-level pulses from 250 fs to sub-10 fs at 38-MHz repetition rate using two gas-filled hollow-core photonic crystal fiber stages

K. F. Mak,[1,*] M. Seidel,[2] O. Pronin,[3] M. H. Frosz,[1] A. Abdolvand,[1] V. Pervak,[3] A. Apolonski,[2,3] F. Krausz,[2,3] J. C. Travers,[1] and P. St. J. Russell[1,4]

[1]*Max-Planck Institute for the Science of Light, Günther-Scharowsky-Str. 1, 91058 Erlangen, Germany*

[2]*Max-Planck Institute of Quantum Optics, Hans-Kopfermann-Str. 1, 85748 Garching, Germany*

[3]*Ludwig-Maximilians Universität München, Am Coulombwall 1, 85748 Garching, Germany*

[4]*Department of Physics, University of Erlangen-Nuremberg, Erlangen, Germany*

**Corresponding author: kafai.mak@mpl.mpg.de*

Received January 6, 2015; revised February 13, 2015; accepted February 16, 2015; posted February 18, 2015 (Doc. ID 231572); published March 18, 2015

Compression of 250-fs, 1-μJ pulses from a KLM Yb:YAG thin-disk oscillator down to 9.1 fs is demonstrated. A kagomé-PCF with a 36-μm core-diameter is used with a pressure gradient from 0 to 40 bar of krypton. Compression to 22 fs is achieved by 1200 fs^2 group-delay-dispersion provided by chirped mirrors. By coupling the output into a second kagomé-PCF with a pressure gradient from 0 to 25 bar of argon, octave spanning spectral broadening via the soliton-effect is observed at 18-W average output power. Self-compression to 9.1 fs is measured, with compressibility to 5 fs predicted. Also observed is strong emission in the visible via dispersive wave generation, amounting to 4% of the total output power. © 2015 Optical Society of America

OCIS codes: (320.5520) Pulse compression; (060.5295) Photonic crystal fibers; (190.5530) Pulse propagation and temporal solitons; (190.7110) Ultrafast nonlinear optics.

http://dx.doi.org/10.1364/OL.40.001238

The latest generation of Yb-based solid-state oscillators, such as those based on thin-disk (TD) geometries, can provide pulses with multi-μJ-level energies at MHz repetition rates, resulting in more than 250 W of average power [1,2]. However, no currently available Yb-doped gain materials are capable of generating few-cycle pulses. Therefore, external pulse compression seems to be the best approach for scaling the high-repetition-rate output to higher peak-power, allowing extreme nonlinear optics such as the generation of high-harmonics and attosecond pulses to be scaled to higher average power. Examples of systems used in external compression include those based on bulk material [3,4], conventional step-index solid glass fiber [5], and gas-filled hollow capillaries [6,7]. The lack of optical guidance in bulk material limits the nonlinear interaction length, and transverse spectral variations across the beam profile can also be an issue. On the other hand, in a solid-core fiber, the maximum peak power is limited to a few MW by material damage and the self-focusing threshold. In contrast, the core diameter of capillaries needs to be greater than ∼150 μm for acceptable optical losses of <3 dB/m. Consequently, peak powers of over 1 GW are necessary in gas-filled capillaries to attain sufficient nonlinear spectral broadening, limiting their application with current generation TD lasers.

Kagomé-structured hollow-core photonic crystal fibers (kagomé-PCFs) present a unique solution for nonlinear spectral broadening. Light is tightly confined within the hollow core and overlaps very weakly with the cladding glass. Consequently, peak powers of over 2 GW can be supported without damage [8]. In addition, transmission losses of ∼1 dB/m over bandwidths of 100 nm can be obtained with core diameters of a few 10 μm. This loss is several orders of magnitude lower than in simple capillary fibers with the same core diameter. Thus, significant intensities and sufficient nonlinearities can be obtained using much lower peak powers without dramatic propagation loss.

While bandgap-guiding hollow-core PCFs have been used for dispersion compensation in pulse compression systems [9] and in soliton self-compression [10], their narrow transmission bandwidth and strongly varying dispersion limit their usefulness in the transmission or generation of few-cycle pulses. Kagomé-PCF, in contrast, offers substantially broader guidance windows, with a waveguide dispersion that is weakly anomalous over the entire wavelength range, so that it can be balanced by the normal dispersion of numerous noble gases at pressures of a few atmospheres [11].

Kagomé-PCFs have previously been used in fiber-mirror compression systems. For example, ∼10 μJ pulses from a 1-kHz Ti:sapphire laser system were compressed from ∼100 to 10 fs [12], and 18-μJ pulses from a 7 MHz TD oscillator were spectrally broadened to support 88-fs pulses [13]. An average power of over 76 W can be reached using such schemes [14]. Alternatively, soliton self-compression, utilizing the weak anomalous dispersion uniquely offered by kagomé-PCF, has also been used to compress ∼7 μJ pulses from a Ti:sapphire amplifier from 24 fs down to 6.8 fs at 790-nm at 1-kHz repetition rate [12], and 35-μJ pulses generated at 1800 nm from an optical parametric amplifier from 80 fs down to 4.5 fs at 2-kHz repetition rate [15].

Here we demonstrate compression of 250 fs pulses from a Kerr-lens mode-locked TD oscillator to sub-10 fs at 38 MHz repetition rate using two gas-filled kagomé-PCF stages as the only nonlinear medium.

The two-stage compression setup is shown in Fig. 1. It is pumped with the Yb:YAG TD oscillator described in

 © 2015 Optical Society of America

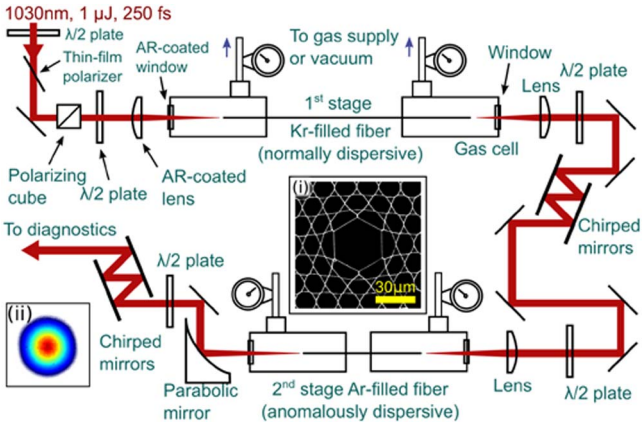

Fig. 1. Schematic of the experimental setup, showing the two fiber stages. Inset (i) scanning electron microscope image of the cross-section of the kagomé-PCF used. Inset (ii) measured transverse profile of output beam.

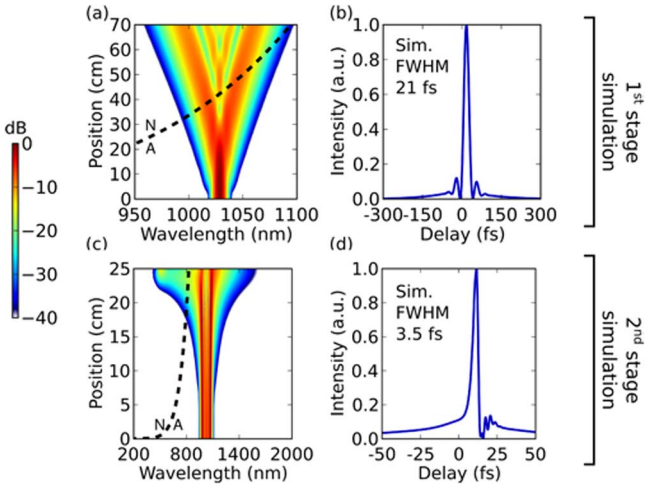

Fig. 2. (a) Numerically simulated propagation of a 250-fs, 0.84-μJ pulse along a 70-cm-long kagomé-PCF with 36-μm core diameter filled with 40 bar Kr at the output gas-cell, and evacuated at the input. The dashed black line indicates the ZDW. (b) Simulated compressed pulse shape based on (a) after 70-cm propagation with GDD optimally compensated. (c) Numerically simulated propagation of (b) through a second 25-cm-long kagomé-PCF filled with 26 bar of Ar from the output end (the front gas cell was also evacuated) at 0.51 μJ, taking account of the dispersion of the window and in-coupling lens. (d) Simulated temporal profile after 23.5 cm of propagation.

detail in [16]. The oscillator delivers 1-μJ, 250-fs pulses at a repetition rate of 38 MHz, corresponding to 40 W of average power. The first stage involves a fiber plus mirror configuration based on self-phase modulation (SPM) under normal dispersion, while the second stage utilizes anomalous-dispersion-assisted self-compression. In each stage, a kagomé-PCF is sealed between two gas cells with independent pressure control. To reduce potential ionization or self-focusing effects and improve coupling into the fiber [17], the input gas cell was continuously evacuated while the filling gas was supplied through the output gas cell. This creates a pressure gradient along the fiber.

The input power was controlled using a half-wave plate and a thin-film polarizer. The transmitted portion from the thin-film polarizer passes through a polarizer cube to increase the polarization extinction ratio (PER) to 25 dB. Light was focused onto the fiber core, through the 3-mm-thick fused-silica (FS) window of the gas cell, using a FS plano–convex lens ($f = 30$ mm). Only the very first input lens and window were anti-reflection (AR) coated for 1030 nm, while the further three windows and two lenses were uncoated. This led to avoidable Fresnel reflection losses of about 30%. Alignment of the input polarization with respect to the eigen-axes of the fiber (which was slightly birefringent) was accomplished using a half-wave plate, thus minimizing coupling between different polarization components and maintaining high intensity along the fiber.

Figure 2(a) shows the numerically-simulated propagation through the first stage, based on the unidirectional full-field nonlinear wave equation [18]. The waveguide dispersion of an evacuated kagomé-PCF is anomalous at all wavelengths, and can be compensated by the normal dispersion of the filling gas. For the kagomé-PCF with 36-μm core diameter used in the experiment, 40 bar of krypton was applied to the output gas-cell, yielding a zero-dispersion wavelength (ZDW)—indicated by the dashed-black-line in Fig. 2(a)—at 1100 nm at the output. The pressure gradient along the 70-cm-long fiber causes the ZDW to shift to higher frequency as one moves closer to the fiber input. Nevertheless, as seen in Fig. 2(a), much of the continuously expanding spectrum is situated in the normal dispersion regime for the section of the fiber beyond 20 cm—where the substantially broadened spectrum is most sensitive to dispersion. Figure 2(b) shows the numerically compressed temporal profile obtained by compensating the output spectrum in Fig. 2(a) using only group-delay dispersion (GDD) compensation, with a pulse duration of 21 fs, and 70% of energy situated within the main peak (defined here as the full-width at the $1/e^2$ points).

The output of the first stage was collimated using an uncoated FS plano–convex lens ($f = 35$ mm). A broadband half-wave plate was used to rotate the polarization back to p-polarization for pulse compression in the double-angle chirped mirrors [19]. The mirrors provided -1200 fs^2 total GDD and no higher-order dispersion compensation. A home-built SHG FROG with a 10-μm-thick BBO crystal and an optical spectrum analyzer were used for pulse characterization. The experimental FROG trace was retrieved well [Figs. 3(a) and 3(b)], and both the directly measured and retrieved spectra extended over 150 nm [Fig. 3(c)]. The retrieved pulse duration was 22 fs [Fig. 3(d)], with 65% of the pulse energy situated within the main peak, in good agreement with the predictions of the numerical simulations and close to the Fourier transform limit of the spectrum [Fig. 3(d), gray circles]. The effects of minor residual 3rd-order dispersion is evident from the asymmetric oscillations at the pulse edge. The output spatial profile was in the fundamental mode [Fig. 1(ii)]. The average power behind the compressor was 28 W. Excluding reflection losses, this corresponds to a transmittance of 80% of the input power.

At full power, the PER was measured to be 16 dB in the case of an evacuated fiber, and 14 dB in the fully pressurized case. The input polarization that yielded optimum extinction ratio differed by up to 15° between the

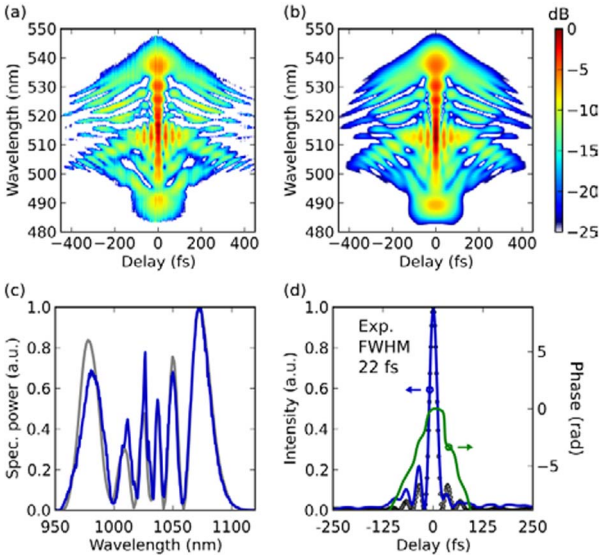

Fig. 3. (a) Experimental SHG-FROG trace at the output of the first stage after -1200 fs^2 chirped mirror GDD compensation and (b) the retrieved SHG-FROG trace. (c) Corresponding measured (blue line) and retrieved (gray line) spectra. (d) Retrieved intensity profile (solid-blue line), phase (solid-green line), and transform-limited pulse profile corresponding to the measured spectrum (gray dots).

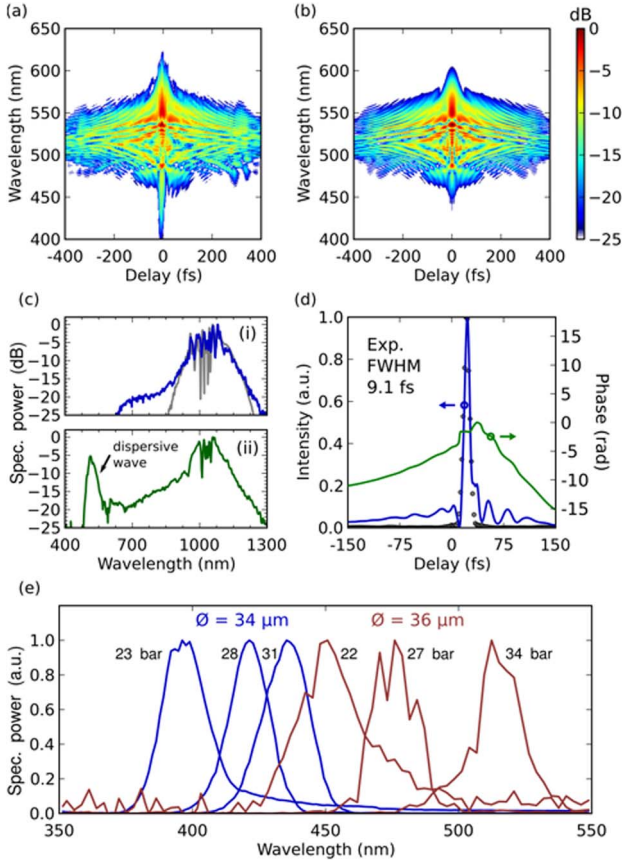

Fig. 4. (a) Experimental SHG-FROG trace of the second fiber output after -210 fs^2 chirped mirror compensation at 26 bar filling pressure and (b) the retrieved SHG-FROG trace. (c)(i) Corresponding measured (blue line) and retrieved (gray line) spectra after the chirped mirrors. (c)(ii) Experimental output spectrum before the chirped mirrors when the Ar pressure is increased to 29 bar so as to enhance the dispersive wave emission. (d) The retrieved intensity (solid-blue line) and phase (solid-green line) profiles corresponding to (c)(i). The Fourier-transform-limited pulse duration for the retrieved spectrum is represented by the gray dots. (e) Experimental tuning of dispersive wave emission via pressure in fibers with 34- and 36-μm core diameters.

evacuated and the pressurized fiber; we attribute this to nonlinear polarization rotation.

The 22-fs output pulse from the first stage was coupled into a second kagomé-PCF, identical to the one used in the first stage, but shorter at 25 cm. It was filled with argon at 26 bar so as to place the ZDW at 808 nm at the fiber output [Fig. 2(c)]. This creates an anomalous dispersion landscape for a pump situated at 1030 nm. Numerical simulations, shown in Figs. 2(c) and 2(d), predict significant soliton-effect self-compression of the input pulse down to a FWHM duration of 3.5 fs directly at the fiber output, with 41% of the energy concentrated within the main peak [Fig. 2(d)]. Due to self-steepening and optical shock formation, a strong spectral extension to shorter wavelengths was also expected.

With the fiber sealed inside a gas cell, the output light must pass through a final gas-cell window (2.3 mm FS). There is also a 2.1-m path through air to the FROG crystal. The resulting extra GDD was compensated using chirped mirrors designed to cancel out the dispersion of fused-silica from 700 to 1300 nm (each bounce compensates for 2 mm of FS). A pair of wedges (~1 mm of fused silica glass in total) was used for fine adjustment. Figures 4(a) and 4(b) show the measured and retrieved FROG traces of the second stage, and (c)–(i) the output spectra, spanning from 1300 nm to at least 700 nm after six bounces off chirped mirrors.

This spectrum (after the chirped mirrors) supports a Fourier-transform-limited pulse of duration ~5 fs. Figure 4(d) shows the corresponding temporal shape of the output pulse, with a retrieved pulse duration of 9.1 fs and 37% of its energy lying within the main peak. The longer pulse duration is likely to be caused by the limited phase-matching available from the 10-μm BBO crystal used, sub-optimal phase compensation by the chirped mirrors at the wings of the spectrum, and incomplete retrieval of the spectral blue tail [Fig. 4(c)(i)]. Coupling efficiencies of around 80% (similar to those obtained in the first stage) were achieved after accounting for reflections from the 6 uncoated surfaces.

The output power at optimal self-compression was 18 W in front of the bare-gold parabolic mirror and 14.5 W after the chirped mirrors. The compression efficiency was about 30%, and could be increased to 45% by AR coating the ten currently uncoated optical surfaces in the system. The PER measured at the second stage output was 13 dB when the fiber was evacuated or pressurized.

The power fluctuations were recorded with a fast photodiode and an oscilloscope. The RF power spectral density (PSD) was calculated by integrating from 10 kHz down to 1 Hz (Fig. 5) and normalizing to the oscillator noise detected in front of the first stage fiber. It shows that the major noise contribution comes from acoustic frequencies at ~100 Hz. An additional peak can also be

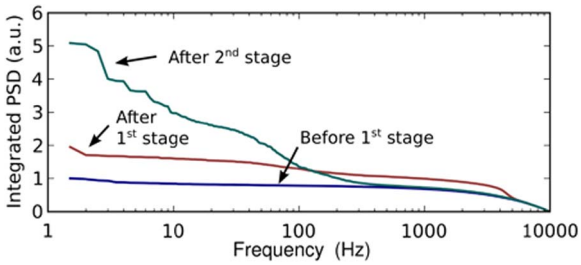

Fig. 5. Noise-PSD after the first and second stages, integrated down from 10 kHz to 1 Hz, normalized to the PSD in front of the first stage.

observed at 4 kHz in the case of slight misalignment. The fluctuations are the strongest when both full power and high pressure are present (28 W output power, in 40 bar of Kr). In contrast, the noise remains low when high power is coupled into an evacuated fiber (0.1 bar), and is only moderately increased when low power (7 W) is coupled into a fiber filled with 40 bar Kr. As in the first stage, the intensity noise increased after propagation through the second fiber (Fig. 5).

A negative-pressure gradient could also be used for soliton self-compression [12], which would allow a window-free output beam path, obviating the need for chirped mirror re-compensation. Light in-coupling would however be hindered at high pressures (26 bar of Ar) and input powers (>20 W).

A characteristic dispersive wave peak at ~500 nm was also present [Fig. 4(c)(ii)] [20]. Since the wavelength of this peak is a function of dispersion and pulse energy, it can be continuously shifted by adjusting the filling gas pressure and input power [Fig. 4(e)]. Dispersive waves at ~400 nm can also be easily obtained by using a kagomé-PCF with a smaller core-diameter of 34 μm [Fig. 4(e)]. The pulse duration of these waves is predicted to be some tens of femtoseconds, depending on the input parameters [20]. To measure the conversion efficiencies, the output light was reflected off four filtering mirrors 99.9% reflective between 370 and 420 nm. At 420 nm [corresponding to the curve with 28 bar Ar in Fig. 4(e)], ~0.5 W was measured, which amounts to 4% of total output power after the second stage. Since the transfer efficiency is higher when the dispersive wave lies closer to the pump in wavelength, the power of dispersive waves near 500 nm should be even stronger.

In summary, 250-fs pulses from a 38-MHz TD oscillator can be compressed in a two-stage kagomé-PCF system, first, using fiber-mirror compression, to 22-fs at 28-W average output power, corresponding to 0.74-μJ pulse energy, and secondly to 9.1 fs (2.7 optical cycles) at 14.5-W average power, using soliton-effect compression. By removing the final chirped mirrors and increasing the gas pressure, a bandwidth spanning 450–1300 nm was also obtained at 18-W average power, with ~4% of the total power concentrated within a tunable emission peak. The scheme presented is compatible with the rapidly increasing power and pulse energies expected from next-generation TD and fiber lasers. Further technical developments, such as improving the thermal stability of the fiber mounts, will be required to maintain the excellent noise properties of the KLM TD oscillator and stabilize the carrier-envelope-phase of the compressed pulses. Numerical modeling suggests that single-cycle pulse durations could be achieved using this approach.

References

1. C. J. Saraceno, F. Emaury, C. Schriber, M. Hoffmann, M. Golling, T. Südmeyer, and U. Keller, Opt. Lett. **39**, 9 (2014).
2. J. Brons, V. Pervak, E. Fedulova, D. Bauer, D. Sutter, V. Kalashnikov, A. Apolonski, O. Pronin, and F. Krausz, Opt. Lett. **39**, 6442 (2014).
3. C. Rolland and P. B. Corkum, J. Opt. Soc. Am. B **5**, 641 (1988).
4. M. Seidel, J. Brons, E. Fedulova, V. Pervak, A. Apolonski, O. Pronin, and F. Krausz, in *Conference on Lasers and Electro-Optics*, Postdeadline Paper Digest (Optical Society of America, 2014), paper STh5 C.9.
5. W. J. Tomlinson, R. H. Stolen, and C. V. Shank, J. Opt. Soc. Am. B **1**, 139 (1984).
6. M. Nisoli, S. De Silvestri, O. Svelto, R. Szipöcs, K. Ferencz, C. Spielmann, S. Sartania, and F. Krausz, Opt. Lett. **22**, 522 (1997).
7. J. Rothhardt, S. Hädrich, A. Klenke, S. Demmler, A. Hoffmann, T. Gotschall, T. Eidam, M. Krebs, J. Limpert, and A. Tünnermann, Opt. Lett. **39**, 5224 (2014).
8. P. Hölzer, W. Chang, J. C. Travers, A. Nazarkin, J. Nold, N. Y. Joly, M. F. Saleh, F. Biancalana, and P. St. J. Russell, Phys. Rev. Lett. **107**, 203901 (2011).
9. J. Limpert, T. Schreiber, S. Nolte, H. Zellmer, and A. Tünnermann, Opt. Express **11**, 3332 (2003).
10. D. Ouzounov, C. Hensley, A. Gaeta, N. Venkateraman, M. Gallagher, and K. Koch, Opt. Express **13**, 6153 (2005).
11. J. C. Travers, W. Chang, J. Nold, N. Y. Joly, and P. St. J. Russell, J. Opt. Soc. Am. B **28**, A11 (2011).
12. K. F. Mak, J. C. Travers, N. Y. Joly, A. Abdolvand, and P. St. J. Russell, Opt. Lett. **38**, 3592 (2013).
13. F. Emaury, C. J. Saraceno, B. Debord, C. Fourcade Dutin, F. Gérôme, T. Südmeyer, F. Benabid, and U. Keller, in *Conference on Lasers and Electro-Optics*, OSA Technical Digest (online) (Optical Society of America, 2014), paper JTh4 J.1.
14. M. Krebs, S. Hädrich, A. Hoffmann, A. Klenke, J. Rothhardt, J. Limpert, and A. Tünnermann, "Compact 10 MHz, 140 MW peak power source enabling bright high harmonic generation," in *Advanced Solid State Lasers Conference*, Shanghai (Optical Society of America, 2014), paper ATu5 A.5.
15. T. Balciunas, C. Fourcade-Dutin, G. Fan, T. Witting, A. A. Voronin, A. M. Zheltikov, F. Gerome, G. G. Paulus, A. Baltuska, and F. Benabid, Nat. Commun. **6**, 6117 (2015).
16. O. Pronin, J. Brons, C. Grasse, V. Pervak, G. Boehm, M.-C. Amann, V. L. Kalashnikov, A. Apolonski, and F. Krausz, Opt. Lett. **36**, 4746 (2011).
17. M. Nurhuda, A. Suda, K. Midorikawa, M. Hatayama, and K. Nagasaka, J. Opt. Soc. Am. B **20**, 2002 (2003).
18. W. Chang, A. Nazarkin, J. C. Travers, J. Nold, P. Hölzer, N. Y. Joly, and P. St. J. Russell, Opt. Express **19**, 21018 (2011).
19. V. Pervak, I. Ahmad, M. K. Trubetskov, A. V. Tikhonravov, and F. Krausz, Opt. Express **17**, 7943 (2009).
20. K. F. Mak, J. C. Travers, P. Hölzer, N. Y. Joly, and P. St. J. Russell, Opt. Express **21**, 10942 (2013).